THE JOURNAL OF BIOLOGICAL CHEMISTRY
Vol. 264, No. 10, Issue of April 5, pp. 5694-5699, 1989
Printed in U.S.A.

Nitric Oxide and Nitrous Oxide Production and Cycling during Dissimilatory Nitrite Reduction by *Pseudomonas perfectomarina**

(Received for publication, August 23, 1988)

Oliver C. Zafiriou‡ and Quentin S. Hanley
From the Department of Chemistry, Woods Hole Oceanographic Institution, Woods Hole, Massachusetts 02543

Gabriella Snyder
From the Division of Applied Sciences, Harvard University, Cambridge, Massachusetts 02138

The denitrifier *Pseudomonas perfectomarina* reduced nitrite under conditions of kinetic competition between cells and gas sparging for extracellular dissolved nitric and nitrous oxides, NO_{aq} and N_2O_{aq}, in a chemically defined marine medium. Time courses of nitrite reduction and NO_g and N_2O_g removal were integrated to give NO_g and N_2O_g yields. At high sparging rates, the NO_g yield was >50% of nitrite–N reduced, and the yield of $NO_g + N_2O_g$ was ~75%. Hence interrupted denitrification yields NO_{aq} and N_2O_{aq} as major products.

The yields varied with sparging rates in agreement with a quantitative model of denitrification (Betlach, M. P., and Tiedje, J. M. (1981) *Appl. Environ. Microbiol.* 42, 1074–1084) that applies simplified Michaelis-Menten kinetics to $NO_2^- \rightarrow NO_{aq} \rightarrow N_2O_{aq} \rightarrow N_2$. The fit gave an estimate of the maximum scavengeable NO_{aq} yield of 73 ± 8% of nitrite–N. Thus a minor path independent of NO_{aq} is also required. The fit of the model to data at lower sparging rates, where normal denitrification products predominate, implies that the extracellular NO_{aq} pool yield is independent of gas sparging rate.

Thus in *P. perfectomarina* NO_{aq} and N_2O_{aq} are intermediates, or facilely equilibrate with true intermediates, during complete denitrification. The recovery of most nitrite–N as NO and/or N_2O under perturbed conditions is not an artifact of irreversible product removal, but an attribute of denitrification in this species, and most probably it is characteristic of denitrification in other species as well.

Payne (1973) proposed a scheme in which the reduction of nitrite to nitric oxide *defined* denitrification:

$$NO_3^- \rightarrow NO_2^- \rightarrow NO \rightarrow N_2O \rightarrow N_2$$

SCHEME 1

Modified or alternative schemes have been advanced for the roles of NO and N_2O in dissimilatory nitrate/nitrite reduction (Zumft and Vega, 1979; Garber and Hollocher, 1981; Payne, 1981a, 1981b; Knowles, 1982) with the most relevant alternative indicating a branch point at an intermediate *X* (Firestone *et al.*, 1979; Averill and Tiedje, 1982):

$$\begin{array}{c} NO_3^- \rightarrow NO_2^- \rightarrow X \rightarrow N_2O \rightarrow N_2 \\ \quad\quad\quad\quad \upharpoonleft\downharpoonright \quad\quad\quad\quad \\ \quad\quad\quad\quad NO \quad\quad\quad\quad \end{array}$$

SCHEME 2

Until very recently, the involvement of unbound NO in any role was primarily an indirect inference from *in vitro* experiments involving various NO reductase activities, as *in vivo* experiments were rendered equivocal by the extreme perturbations involved, such as very high cell densities (Garber and Hollocher, 1981) or presence of inhibitors or detergents (Firestone *et al.*, 1979; Betlach and Tiedje, 1981). However, Goretski and Hollocher (1988) have now demonstrated that unbound NO clearly plays some important role(s) in denitrification by several species of denitrifiers. Using extracellular hemoglobin (Hb) as a trap under *irreversible* conditions, these authors typically trapped 60–70% of the nitrite–N reduced by intact cells as HbNO at high [Hb].

Here we report experiments confirming the importance of extracellular NO and N_2O for the marine species *Pseudomonas perfectomarina*, implying that marine denitrifiers may be an important source and/or sink of the NO observed in suboxic marine environments (Goering, 1985; Ward and Zafiriou, 1988).[1] Furthermore, our method of detecting NO and N_2O evolution in the presence of a kinetically defined alternative sink, permitting measurements under *partially reversible* conditions, gives a more complete view of the full sequence of events envisioned in Schemes 1 and 2.

We estimate the availability of NO_{aq} and N_2O_{aq} outside the cell by bubbling denitrifying cell suspensions with a gas stream and measuring the volatilized products NO_g and N_2O_g in the effluent gas stream. We assume that the bubbling process has no direct effect on the cellular emission or uptake of these gases. Using this approach, we 1) measure the yields of NO_{aq} and N_2O_{aq} as functions of physical removal rate, 2) model the competition between physical removal and reuptake in order to derive limiting yields at infinite physical removal rate, and 3) evaluate the results in terms of Schemes 1 and 2.

MATERIALS AND METHODS[2]

RESULTS

Experimental Design and Kinetic Scheme—Experiments utilized anaerobic batch cultures of *P. perfectomarina* in a

* This work was funded by National Science Foundation Grants OCE-83-00022 and OCE-86-01618. This is Woods Hole Oceanographic Institution Contribution 6509. The costs of publication of this article were defrayed in part by the payment of page charges. This article must therefore be hereby marked "*advertisement*" in accordance with 18 U.S.C. Section 1734 solely to indicate this fact.
‡ To whom correspondence should be addressed.

[1] O. C. Zafiriou, submitted for publication to *Nature*.

[2] Portions of this paper (including "Materials and Methods," Table 3, Fig. 5, and equations and supporting data) are presented in miniprint at the end of this paper. Miniprint is easily read with the aid of a standard magnifying glass. Full size photocopies are included in the microfilm edition of the Journal that is available from Waverly Press.

chemically defined marine medium under nitrogen with succinate as carbon source, excess ammonia available for N assimilation, and nitrite at oceanically relevant concentrations as limiting electron acceptor. A computer-controlled experimental and data acquisition system continuously sparged the media with oxygen-free N_2 at known, reproducible rates and quantified NO and N_2O in the effluent gases over the time course of nitrite respiration. Sterile media were used as controls. The system frequently recalibrated the detectors to optimize accuracy. Rate laws and constants for transfer (sparging) of dissolved NO and N_2O from sterile media into the gas phase were determined in separate experiments.

The yields of gases removed were determined by integrating over the time courses of their evolution. The total yields over the course of nitrite exhaustion are the quantities reported. The data from a series of experiments at various gas flow rates were fitted to a kinetic approximation (Miniprint Supplement) derived from Scheme 3:

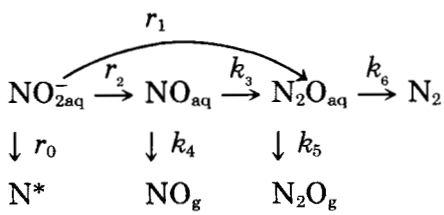

SCHEME 3

Scheme 3 is an elaboration of Schemes 1 and 2. Following Betlach and Tiedje (1981), we 1) assume that NO_{aq} and N_2O_{aq} are in steady state, controlled by Michaelis-Menten kinetics, 2) add the competing physical removal pathways introduced by bubbling with gas, and 3) allow for both direct reduction to N_2O (Zumft and Vega, 1979) and unknown losses, N*, presumably by N assimilation or "direct" N_2 formation. Reduced nitrite-N initially partitions in fixed proportions among $NO_{aq}(r_2/\sum r)$, NO_{aq}-independent N_2O_{aq} $(r_1/\sum r)$, and other fates $(r_0/\sum r)$. NO_{aq} formation (r_2) is balanced by physical (k_4) and biological (k_3) removal; likewise, N_2O_{aq} production by r_1 and k_3 is balanced by k_5 and k_6 terms.

Time Course and Flow Dependence of Gas evolution—Fig. 1 shows a typical experiment. After a brief lag, nitrite was reduced to undetectable levels at a nearly constant rate. In near synchrony, NO_g and N_2O_g concentrations rose to similar plateaus and then declined to undetectable levels. Cell numbers increased only slightly, primarily after nitrite was depleted. At higher nitrate concentrations, or during aerobic respiration, cell numbers increased rapidly, but at oceanically relevant nitrite levels (0–20 μM) growth was slow. Slow growth does not imply senescence or damage by bubbling, as cells were capable of rapid aerobic growth at the end of gas evolution, bubbled and unbubbled cultures reduced nitrite at similar rates, and replenishment of nitrite immediately after its exhaustion initiated a second, similar time course. Bubbling did not cause detectable cell aggregation or decrease cell counts. Additional experiments (Miniprint Supplement) showed that qualitatively similar results are found when inoculation, medium composition, and other parameters are varied.

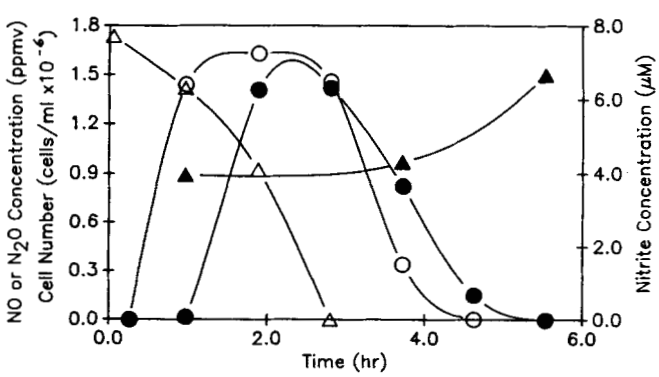

FIG. 1. **Typical time course of $[NO_2^-]$ (△——△), cell density (▲——▲), NO (○——○), and N_2O (●——●) in the effluent gas stream, 0.25 liter (standard temperature and pressure)/min N_2.**

The results of 14 experiments at various flows (Table 1) qualitatively establish several major points. In unbubbled cultures NO_{aq} did not build up; <0.2% of the nitrite reduced was present as NO_{aq} (not shown). The NO yields from bubbled cultures ranged from 11 to 63% and tended to increase with increasing bubbling rate. The errors are large enough that it is unclear whether a plateau value for the NO_{aq} yield was achieved at high gas flows. The N_2O yields, which ranged from 26 to 42% of nitrite-N, showed a maximum at intermediate bubbling rates. This intermediate maximum is expected from Scheme 3 because at low gas flow N_2O_{aq} removal as N_2O_g competes poorly with uptake and reduction, while at high flow most of the precursor, NO_{aq}, is physically removed as NO_g.

These experiments establish directly that purgeable NO_{aq} and N_2O_{aq} are involved in the major, possibly the only, reductive N pathway under our conditions. Over half of the nitrite reduced could be recovered as NO, and at the highest flows the total recovery of gaseous N compounds averaged 73 ± 8%. The major question thus became whether extracellular yields approach 100% or some lower value implying the necessity for additional, NO_{aq}-independent pathways.

Parameters of Scheme 3—Fitting the data to Scheme 3 yielded an evaluation of its suitability and a more quantitative estimate of partitioning of reduced N among various pathways. First, we verified the reasonableness of our simplification of the full Michaelis-Menten kinetics (zero order uptake of nitrite, first order uptake of dissolved gases) by comparing Michaelis-Menten K_m values of substrates with their concentrations in the medium. Table 1 gives initial nitrite concentrations and estimates of the dissolved gas concentrations. Figs. 2 and 3 show K_m estimates for nitrite and NO_{aq}. As required, the apparent K_m for nitrite was well below the nitrite concentrations for >90% of the time courses and the K_m for NO_{aq} was well above the estimated values of $[NO_{aq}]$. K_m (N_2O) was not measured; however, Betlach and Tiedje (1981) reported a value of 540 nM, more than twice the highest estimated $[N_2O_{aq}]$ and 10-fold above its average concentration in our experiments.

To evaluate the likely degree of distortion in the r and k terms of Scheme 3 if our kinetic approximations are significantly in error, we also calculated results assuming drastically different NO_{aq} uptake kinetics. The best-fit parameters found using the approximations (justified above) of zero-order nitrite reduction and first-order uptake of NO_{aq} and N_2O_{aq} are given in Table 2 (top line). The second line presents the results calculated assuming uptake second-order in $[NO_{aq}]$ (Miniprint Supplement). The resulting values for $r_2/\sum r$, 73 ± 8% for first-order NO_{aq} uptake *versus* 63 ± 5% for second-order NO_{aq} uptake, indicate that the NO yields are very insensitive to uptake order. Assuming zero-order NO uptake kinetics (as would result from saturated Michaelis-Menten uptake) predicts an NO yield independent of flow rate and is clearly inappropriate (Fig. 4).

The flow rate–gas yield behavior predicted from the best-

TABLE 1
Nitrite dissimilation experiments

Flow rate[a]	Initial $[NO_2^-]$	$d[NO_2^-]/dt$[b]	Cells[c]	NO and N_2O concentrations						
				Recoveries[d]			Gaseous[e]		Solution[e]	
				NO recovery	N_2O recovery	Total recovery	$[NO]_{max}$	$[N_2O]_{max}$	$[NO_{aq}]_{ss}$	$[N_2O_{aq}]_{ss}$
liters/min	*μM*	*nM/s*	*ml (× 10^{-6})*	%	%	%	*ppm*		*nM*	
0.15	12.8	0.88	0.5	11.2	27.6	38.8	1.39	2.24	55.2	180
0.15	12.6	0.98	1.2	23.5	25.2	48.8	1.96	2.34	61.5	200
0.18	8.2	0.45	1.1	—[f]	39.8	—[f]		1.47	26.6	77
0.25	12.3	1.12	2.4	37.7	36.1	73.8	2.91	2.27	58.7	136
0.25	7.7	0.60	0.89	23.7	40.8	64.5	1.63	1.32	31.5	73
0.35	8.2	0.45	1.4	—[f]	42.0	—[f]	—[f]	0.79	20.4	37
0.50	8.2	0.32	1.8	43.4	34.5	77.9	0.52	0.32	11.9	16
0.50	10.9	0.45	2.9	49.2	27.2	76.4	0.87	0.37	16.9	23
0.50	7.6	0.58	1.2	39.3	32.0	71.3	1.00	0.55	21.9	30
0.50	11.4	0.85	1.9	37.9	33.6	71.5	1.14	0.75	32.0	43
0.56	11.7	0.73	1.2	39.4	26.1	65.5	0.82	0.60	25.8	32
1.00	12.2	0.78	2.5	47.7	25.8	73.5	0.59	0.31	17.6	13
1.50	7.4	0.45	1.2	50.5	—[f]	—[f]	0.30	—[f]	7.9	4.0
1.50	8.7	0.48	0.9	63.3	—[f]	—[f]	0.48	—[f]	8.5	4.3

[a] Dry gas at standard temperature and pressure.
[b] Zero-order rate over central >80% of progress curve.
[c] Initial values; increase <40% before nitrite exhaustion.
[d] As percent of added nitrite–N.
[e] Gas values measured; solution values derived from calculation in Miniprint Supplement.
[f] Not measured.

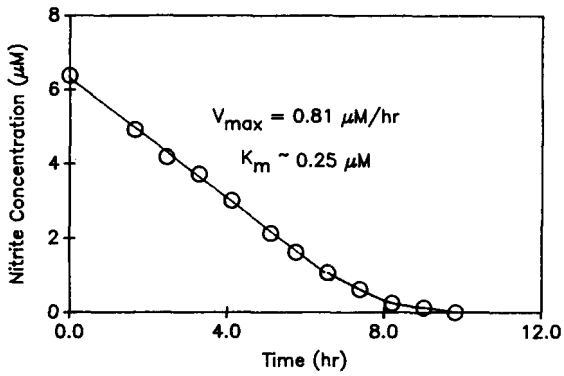

FIG. 2. **Nitrite uptake by *P. perfectomarina* and derived estimates of Michaelis-Menten parameters.** Intensive sampling of medium from a culture being sparged at 200 ml (standard temperature and pressure)/min N_2.

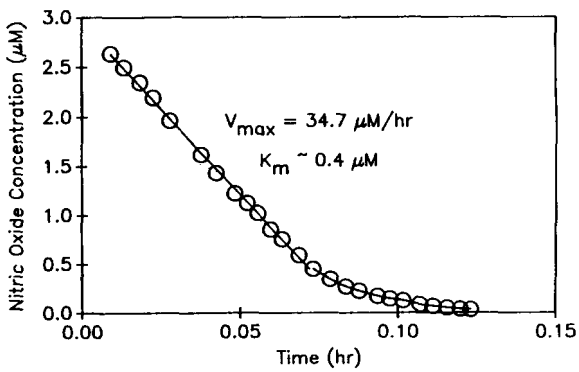

FIG. 3. **NO_{aq} uptake by *P. perfectomarina* and derived estimates of Michaelis-Menten parameters.** An anaerobic *P. perfectomarina* culture in a 2-liter headspace-free syringe was spiked with ~4 μM NO_{aq} in the presence of 100 μM $[NO_2^-]$, and the mixture was pumped at a constant rate into a gas-stripping device coupled to the NO detector, permitting continuous measurement of $[NO_{aq}]$ *versus* time.

fit parameters is shown in Fig. 4 along with the data. The features identified qualitatively above, a maximum in N_2O yield and an asymptotic behavior of NO yield, are reproduced at intermediate flow, as shown by the best-fit lines. The value of r_2, the asymptote of the integrated NO yield at high flow, is 73 ± 8%. Although the reliability of this value is imprecisely known, the uncertainties seem too small to accommodate a value of 100% for r_2. Hence we conclude that most, *but not all* of the nitrite–N reduced is purgable as NO_{aq}. Using external Hb as a trap, Goretski and Hollocher[3] also found the rates of HbNO formation rates at high [Hb] for *P. Perfectomarina* to be about 65% of nitrite reduction obtained in separate experiments.

The fate of the remaining $(100 - r_2)$% of nitrite–N reduced is uncertain. Although the value of r_0 is greater than that of r_1 (Table 2), its uncertainty is very large, casting doubt on its significance. That r_0 is likely zero is also consistent with the richness of the medium in ammonia–N for assimilation, the most likely sign of the calibration error for N_2O_g (Miniprint Supplement), and the absence of any published evidence for direct N_2 formation. Thus r_1, the "direct" path to N_2O_{aq}, is thought to be the second most significant term required by the data and Scheme 3.

The value of k_3, the rate constant for cellular uptake of NO_{aq}, is also significantly above zero. Hence *under precisely the same conditions and contemporaneously with its evolution*, NO_{aq} is consumed biologically. The two-parameter emission-uptake fit (Fig. 4) for NO_{aq} has an r^2 value 0.9, and hence is a good quantitative description of the data. Although we present and analyze the integrated time courses here, examination of the temporal patterns also shows that stepwise evolution and temporally discrete reduction of these intermediates is not a major process, in agreement with the analysis of Betlach and Tiedje (1981).

The results for N_2O_{aq} show a "direct" path yielding about 11% of total reduced N as N_2O, representing at most about one-quarter of the total N_2O yield. Hence most N_2O derives from NO_{aq} via the $r_2 - k_3$ sequence. The N_2O_{aq} uptake rate

[3] T. C. Hollocher, personal communications.

TABLE 2
Parameters fit to Scheme 3

NO uptake order assumed	Fates of nitrite-N[a]			Uptake of NO_{aq} and N_2O_{aq}[b]		Physical gas removal kinetics[c]	
	r_0	r_1	r_2	k_3	k_6	k_4	k_5
					s^{-1}	$s^{-1}\ F^{-1}$	
1	16.1 ± 12	10.8 ± 4	73.1 ± 8	0.0083 ± 0.002	0.001 ± 0.0003	0.0221 ± 0.007	0.0103 ± 0.0002
2			62.6 ± 5	0.031 ± 0.007		0.0221 ± 0.007	0.0103 ± 0.0002

[a] Percent of nitrite–N.
[b] For first-order uptake values in s^{-1}; for second-order uptake $nM^{-1}\ s^{-1}$.
[c] Apparatus-dependent physical removal rates of dissolved gases measured in sterile medium. F is gas flow at standard temperature and pressure in liters/min.

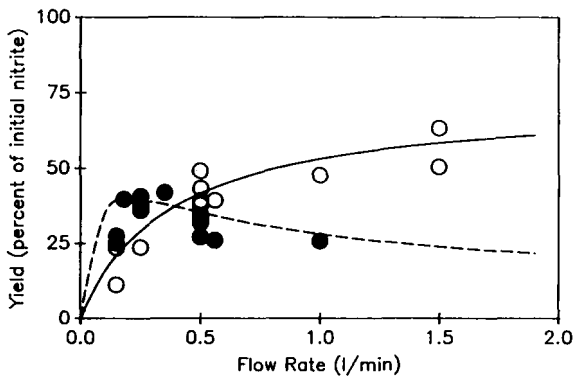

FIG. 4. **Predicted (*lines*) and experimental integrated yields of NO_g (○——○) and N_2O_g (●– – –●) as functions of bubbling rate.** Data from Table 1, curves from Scheme 3, and equations in Miniprint Supplement.

constant is also greater than zero, demonstrating simultaneous N_2O production and uptake. The N_2O_{aq} uptake rate constant is nearly an order of magnitude smaller than that for NO_{aq}.

In summary, the data are consistent with the model represented in Scheme 3. Most but not all nitrite–N reduced becomes available as extracellular NO_{aq}, which is largely taken up and reduced further to N_2O_{aq}. This N_2O_{aq} is also available for further reduction. Only about 11% of the N_2O–N, a quarter of the total, appears to be produced by "direct" $NO_2^- \rightarrow N_2O$ path that circumvents NO_{aq}. Goretski and Hollocher (1988) likewise found that a component of N_2O production could not be eliminated by high concentrations of the extracellular NO trap Hb.

DISCUSSION

The principal question previously posed has been whether or not NO (location unspecified) is an "obligate-free intermediate" (Payne, 1981b; Garber and Hollocher, 1981). The best currently achievable operational criterion for "free" appears to be "extracellular," as demonstrated by Hb trapping (Goretski and Hollocher, 1988) or gas-liquid equilibration. Such experiments clearly define free extremely rigorously, since without doubt intracellular free intermediates also exist. The striking result is that a large fraction of the reduced N flux satisfies this rigorous criterion, testifying to the power of the constraint. The isotopic experiment of Firestone *et al.* (1979) also indicated a free pool of very similar size to the extracellular one described here; it was not demonstrated that the trapping was fully saturated.

Since species in facile equilibrium with a true intermediate are difficult to distinguish from the intermediate itself, we cannot differentiate between Schemes 1 and 2, although NO is mechanistically a true intermediate in 1 and not in 2. Both schemes permit NO and N_2O to satisfy necessary (but not sufficient) criteria for an intermediate: 1) presence, shown by trapping, 2) antecedency to products, shown by diminished product yields upon removal from and/or enhanced yields upon addition to a reacting system.

Extracellular NO as a Product—Equating "NO_{aq}" to gas- or Hb-scavengeable, extracellular NO is justified by the absence of mechanisms for these processes to influence intracellular pools directly. However, the external NO sink indirectly perturbs intracellular pools by inducing a net diffusive flux from the cell, as analyzed in detail in the Appendix of Goretski and Hollocher (1988). The experiment of these authors establishes that at the limit of maximal trapping (scavenging rate constant for NO_{aq} approximately 1000–5000/s) this net induced flux is ~65% of the nitrite reduced in the case of *P. perfectomarina*.[3] This proves that HbNO can become the major *product* of the reaction and opens the question of whether the extreme conditions have "sucked out" NO in an entirely unnatural manner. Our experiments at high flow and extrapolation to infinite flow rates showed similar limiting product (NO_g) yields as the HbNO yields of Goretski and Hollocher (1988) even though our scavenging rate constant was about 100,000 times lower, corresponding to NO residence times in solution of several minutes. This correspondence of yields under greatly differing conditions, using different trapping methods, suggests that operationally the definition of "extracellular" is robust. Our trapping timescale is also sufficiently slow to suggest that in nature environmentally realistic chemical and biological NO sinks may provide alternative fates.

NO and N_2O_{aq} as Intermediates—Although under strong perturbation NO_{aq} and N_2O_{aq} are major products of nitrite reduction, these maximum product yields may not be valid estimates of the role of NO_{aq} (and N_2O_{aq}) as intermediates in balanced denitrification ($1\ NO_2^- \rightarrow$ ~½ N_2). Cells switching from N_2 to NO as their principal product are deprived of about half (⅔ × 73%) of the supply of electron acceptors and of N species reduced beyond the 2+ level, potentially eliciting chemical or regulatory feedbacks not included in Scheme 3. However, the kinetics predicted by Scheme 3 fit the data from all our experiments (Fig. 4), which involved removal of from 10–85% of the limiting NO yield, hence ranging from almost unperturbed NO_{aq} intermediacy to almost complete trapping as product.

The simplest interpretation of this fit is that the assumed constancy of the r and k terms of Scheme 3 is correct: limiting yields do represent degree of intermediacy in balanced denitrification as well. While uncertainties permit some undetected variations in these parameters, drastic shifts are not consistent with the fit of Fig. 4. To our knowledge, this is the first direct demonstration of this important point for both of these species under identical conditions.

Analogous arguments apply to N_2O cycling in principle. However, "obligate-free intermediacy" is generally accepted for N_2O, and our own results show a much smaller first-order

uptake rate for N_2O_{aq} than for NO_{aq} (Table 2, k_3 *versus* k_6). Hence the principal new information we derive is that a large fraction of N_2O derives from NO_{aq}.

Mechanism of Denitrification—These results establish three important points, which the data of Goretski and Hollocher (1988)[3] imply may be general, rather than peculiar to *P. perfectomarina*. First, unequivocally extracellular NO and N_2O can become the stoichiometrically dominant products. Second, *simultaneous* concurrent production and consumption of NO_{aq} and N_2O_{aq} appear to occur with similarly large extracellular components under conditions of complete denitrification, thus realizing the sequence model led by Betlach and Tiedje (1981) in a real cellular system. Finally, individual steps in our scheme have previously been studied using extremely high cell and reagent concentrations and in very short-term experiments. The fact that our cultures fit Scheme 3 at near-natural substrate levels for relatively long periods and repeat their time course behavior on replenishment of nitrite, strongly suggests that this scheme may approximate denitrification by *P. perfectomarina* in nature.

Ecological Implications—The facile evolution and uptake of NO from *P. perfectomarina* and other denitrifiers suggests a strong interaction between these organisms and their environment with respect to release of NO, with implications regarding the cycling of N, the ultimate fate of NO, and the origin of N_2O in denitrifying systems. Competition among cells and species for extracellular NO is a logical inference, and chemical sinks may also be important for extracellular NO, possibly diverting formally "denitrified" N (*e.g.* NO) (Payne, 1981a, 1981b) to products other than N_2O or N_2. The detection of rapidly cycling NO in the suboxic regions of the oceanic water column (Goering, 1985; Ward and Zafiriou, 1988)[1] suggests that these paths require consideration in that environment.

Acknowledgments—We thank Drs. N. V. Blough, T. C. Hollocher, T. T. Packard, and J. Waterbury for fruitful discussions, Dr. E. Sholkovitz for software advice, and M. B. True and F. Valois for technical assistance.

REFERENCES

Averill, B. A., and Tiedje, J. M. (1982) *FEBS Lett.* **138,** 8–12
Baumann, P., Bowditch, R., Baumann, L., and Beaman, B. (1983) *Int. J. Syst. Bacteriol.* **33,** 857–865
Bennett, M. R., Brown, G. M., Maya, L., and Posey, F. A. (1982) *Inorg. Chem.* **21,** 2461–2468
Betlach, M. R., and Tiedje, J. M. (1981) *Appl. Environ. Microbiol.* **42,** 1074–1084
Firestone, M. K., Firestone, R. B., and Tiedje, J. M. (1979) *Biochem. Biophys. Res. Commun.* **91,** 10–16
Garber, E. A. E., and Hollocher, T. C. (1981) *J. Biol. Chem.* **256,** 5459–5465
Goering, J. J. (1985) in *Denitrification in the Nitrogen Cycle* (Golterman, H. L., ed) NATO Conference Ser. I, pp. 191–224, Plenum Publishing Corp., New York
Goretski, J., and T. C. Hollocher (1988) *J. Biol. Chem.* **263,** 2316–2323
Hobbie, J. E., Daley, R. J., and Jasper, S. (1977) *Appl. Environ. Microbiol.* **33,** 1225–1228
Knowles, R. (1982) *Microbiol. Rev.* **46,** 43–70
Payne, W. J. (1973) *Bacteriol. Rev.* **37,** 409–452
Payne, W. J. (1981a) in *Denitrification, Nitrofication, and Atmospheric Nitrous Oxide* (Delwiche, C. C., ed) pp. 85–103, Wiley-Interscience, New York
Payne, W. J. (1981b) *Denitrification*, Wiley-Interscience, New York
Payne, W. J., Riley, P. S., and Cox, C. D., Jr. (1971) *J. Bacteriol.* **106,** 356–361
Rhodes, M. E., Bost, A. N., and Payne, W. J. (1963) *Can. J. Microbiol.* **9,** 799–807
Strickland, J., and Parsons, T. (1965) *A Practical Handbook of Seawater Analysis*, 2nd Ed., Vol. 125, Bulletin of the Fisheries Research Board of Canada, Ottawa
Ward, B. B., and Zafiriou, O. C. (1988) *Deep-Sea Res.* **35,** 1127–1142
Weiss, R. F. (1981) *J. Chromatogr. Sci.* **19,** 611–616
Yoshizumi, K., Aoki, K., Matsuoka, T., and Asakura, S. (1985) *Anal. Chem.* **57,** 737–740
Zumft, W., and Vega, J. (1979) *Biochim. Biophys. Acta* **548,** 484–499

SUPPLEMENTARY MATERIAL TO:
Nitric Oxide and Nitrous Oxide Production during Dissimilatory Nitrite Reduction by Pseudomonas perfectomarina
Oliver C. Zafiriou, Quentin S. Hanley and Gabriella Snyder

1. Cells, Inocula, Media

P. perfectomarina (ATCC #14405, Baumann et al., 1983) was maintained aerobically on agar plates (1%) of the same chemically defined medium used in liquid form for the experiments (375 ml of 0.2 μm Nucleopore filtered coastal seawater of salinity 30‰, 1.0 g sodium succinate, 0.62 g ammonium sulfate, 0.25 g $NaHCO_3$, 5.8 mg K_2HPO_4, 1 mg chelated Fe, 0.5-1 mg $NaNO_2$, 200 μg $MnCl_2$, 100 μg Na_2MoO_4, 100 μg $ZnSO_4$, 20 μg $CuSO_4$, and 2 μg $CoCl_2$, diluted to 1 liter with Milli-Q deionized water). Its pH after autoclaving was 8.3. After initial degassing, the sterile medium neither produced nor consumed detectable amounts of NO or N_2O.

Single colonies were transferred from agar plates to aerobic liquid medium, incubated until turbid, and stored at 5°C. Inocula were prepared from this culture by transferring small aliquots into fresh liquid medium, allowing growth to an optical density of ~0.1 per cm at 425 nm (mid to late-$\log_e$ phase) and inoculating pre degassed media to the desired cell density. Inocula were checked randomly for contamination; none was detected.

Anaerobic conditions alone induce synthesis of denitrifying enzymes in *P. perfectomarina* (Payne et al., 1971) and in simple media asparagine is required for growth (Rhodes et al., 1963). Several experiments demonstrated that anaerobic inocula or alternative carbon sources, including asparagine, resulted in qualitatively similar NO recoveries to those reported in Table 1, despite the fact that suboptimal gas flow rates were utilized. Additionally, a single experiment utilizing *Ps. denitrificans* gave a large NO yield as well, in agreement with the result of Goretski and Hollocher (1988) (Table 3). Thus large NO yields are not unique to a single organism or inoculation condition, and are not coupled to cellular growth.

2. Experimental Incubations

Incubations were initiated by rigorously degassing 1.5 liters of sterile medium in four 2-liter Pyrex bottles with 99.999% N_2, inoculating three bottles to an estimated 1.2×10^6 cells/ml and retaining the fourth as a sterile control. Bottles were bubbled at constant flow rate, F, (ml/min STP) while being sampled or analyzed for cell density, nitrite concentration, and the NO and N_2O content of the effluent gases under the control of a computerized data acquisition and control system described below. Incubations were continued until concentrations of all measured N compounds were below the limit of detection for at least two consecutive measurements. The gaseous NO and N_2O concentrations times N_2 flow rates gave 6-10 gas evolution rates during a time course (e.g., Fig. 1) which were integrated by the trapezoid rule to give the moles of N evolved and divided by the number of moles of nitrite per flask to give yields (Table 1).

3. Sampling and Chemical Analyses

The gas analysis system was repetitively calibrated using standard gas mixtures during each experiment. Aliquots of the liquid for subsequent colorimetric nitrite determination (Strickland and Parsons, 1965) and cell counts (acridine orange stained cells on Irgalen black stained 0.2 μm Nucleopore filters (Hobbie et al., 1977)) were pumped into test tubes containing a drop of formalin as preservative.

Effluent gases were partially dehumidified by passage through traps at -40°C. The gas stream selection valve connected the appropriate experimental or standard gas mixture to a 1.8 ml gas sample injection loop for N_2O analysis on a Shimadzu GC-8A equipped with 2.5 m X 3 mm column (molecular sieve 5A, 60/80 mesh) for separation of CO_2 and N_2O at 280°C and N_2O detection by ^{63}Ni electron-capture detection at 350°C (Weiss, 1981). *Carrier gas was* 99.999%, Linde N_2 or Linde P-10 argon-methane at 40-60 ml/min.

The N_2O detection system was calibrated several times per experiment by interspersing standards with samples, using 1, 2, and 3 ppmv gas standards generated by dynamic dilution of Scott 25.01 ppmv N_2O/N_2 by a mass flow controller system. The resulting peak heights were fitted to a 4-point regression curve which was used to convert peak heights into concentrations. An independent absolute calibration was carried out using an aqueous N_2O standard generated by the reaction of stoichiometrically limiting hydroxylamine with excess nitrous acid (Bennett et al., 1982). This comparison gave N_2O values 89% of those calculated using the gas standard. The reported N_2O values are 0.89 times the gas standardization value.

The NO content of standards and experimental gas streams was quantified by admitting 125 ml/min of gas into a Monitor Labs Model 8840 NO_x chemiluminescence-type detector in the NO mode. Standards were prepared as for N_2O by dynamic dilution of a 100 or 200 ppmv NO/N_2 standard (Airco) to levels in the 0-3 ppmv NO range. The regressions of measured peak height vs NO concentration in standards typically exhibited standard errors of 0.02 ppmv, corresponding to a statistical uncertainty of about 0.7% full-scale. The working gas standard was compared to an absolute NO_{aq} standard prepared by the reaction of stoichiometrically limiting nitrous acid with excess iodide in aqueous acid iodide (Yoshizumi et al., 1985). The aqueous standard indicated 111.4% of the NO values based on the working gas standard. The reported results are 1.114 times those based on the working gas standard.

4. **Application of Scheme 2 to Cell Suspensions**

The kinetic scheme can be applied to time-course culture experiments by deriving equations that require the following information and assumptions (1) gas removal kinetic form and rate constants, (2) mass balance for stoichiometrically important N species, (3) relationship between $[S]_g$ and $[S_{aq}]$ (S is a dissolved gas), and (4) kinetic expressions for the biological transformations combined with the steady-state assumption for the transient species NO and N_2O. These are incorporated in a standard treatment of parallel and consecutive reactions.

The physical removal of dissolved gas S from bubbled media depend on its solubility, concentration $[S_{aq}]$, the stripping gas flow rate F, and factors constant in our experiment, such as the size and pore distribution of the frit used, the shape and stirring of the vessel, temperature, and gas-phase dead volume between solution and detector. Invariant factors are subsumed in the constant in the rate law for physical removal of dissolved gas:

$$-d[S_{aq}]/dt = k_s[S_{aq}]F, \quad \text{where } F = \text{gas flow rate}$$

We verified this relationship and determined the required stripping rate constants in a series of experiments at different flow rates. In each experiment the stripping gas flow rate was constant. Sterile medium was spiked with NO_{aq} or N_2O_{aq}, and the time course of spike concentration in the gas was determined at intervals of 5-10s (NO) or 300-350s (N_2O) until baseline values were obtained. The exponential concentration-time curves yielded corresponding first-order rate coefficients whose regression against F gave the expected linear relationships and whose slopes gave the values of k_{NO} and k_{N_2O} in Table 1 (Fig. 5).

The mass balance equation for stoichiometrically important N species at time t is:

$$\text{Total N} = (NO_2^- - N)_{initial} = (NO_2^- - N)_t + (NO - N)_t + (N_2O - N)_t + (N^*)_t.$$

The dissolved gas concentrations, $[NO]_{aq}$ and $[N_2O]_{aq}$, are the substrate concentrations for biological uptake kinetics. We measured directly only gas-phase values, $[NO]_g$ and $[N_2O]_g$. The aqueous values subscripted as "steady state" in Table 1 were obtained from the steady state approximation given below. The reasonableness of these values is confirmed by calculating the dissolved gas concentrations in solubility equilibrium with the medium from the known gas-phase concentrations and Henry's Law constants. The equilibrium solubility values are smaller than the steady-state values by a factor of about 5, in accord with other data showing that the effluent is ~10% equilibrated with the solution.

Deriving the steady-state kinetic equations requires suitable kinetic forms for the various biological steps; e.g., Betlach and Tiedje (1981) used a full Michaelis-Menton treatment for each step. For simplicity we reduced each step to a suitable approximation of that treatment (saturation - zero order, or low substrate - first order) for each substrate.

Zero order kinetics for nitrite uptake were used since the measured nitrite reduction rates in each run approximated zero order, and a time course fit to the Michaelis-Menton equation gave a Km of 0.25 μM (Fig. 2), well below the substrate concentration for the initial 90% of the reactions.

For NO and N_2O, first-order biological uptake kinetics give:

$$[NO]_{ss} = \frac{r_2(dNO_2^-/dt)}{k_3 + k_4F}$$

$$[N_2O]_{ss} = \frac{k_3[NO]_{ss} + r_1(dNO_2^-/dt)}{k_5F + k_6}$$

$$\text{Yield (NO)} = \frac{r_2k_4F}{k_3 + k_4F}$$

$$\text{Yield } (N_2O) = \frac{r_1k_5F}{k_5F + k_6} + \frac{r_2k_3k_5F}{(k_3 + k_4F)(k_5F + k_6)}$$

No direct measurements are available to support the assumption of first-order uptake for N_2O, but the only available estimate of $K_m(N_2O)$, 540 nM (Betlach and Tiedje, 1981), is well above the $[N_2O]ss$ we derive (Table 1). For NO, the Km estimate for Figure 3, 400 nM, is likewise consistent with a first-order treatment given the dissolved gas values in Table 1. However, to ensure that the calculated values were not extremely sensitive to the assumed order in NO, we formulated equivalent equations assuming zero-order NO uptake (saturated Michaelis-Menton) or second-order uptake (rate-limiting dimerization to form an N_2O precursor). For zero-order NO uptake:

$$[NO]_{ss} = \frac{r_2(dNO_2^-/dt) - k_3}{k_4}$$

As discussed in the text, zero-order NO uptake gives no dependence at $[NO]_{aq}$ on F, in contrast to the data (Table 1, Fig. 4).

For second-order NO uptake:

$$[NO]_{ss} = \frac{-k_4 \pm \sqrt{k_4^2 + 4k_3r_2\, d(NO_2^-)dt}}{2k_3}$$

Second-order yield expressions are:

$$\text{Yield(NO)} = \frac{r_2k_4F[NO]_{ss}}{k_4F[NO]_{ss}} + k_3$$

$$\text{Yield}_{N_2O} = \frac{r_1k_5F[N_2O]_{ss}}{k_5F[N_2O]_{ss} + k_6} + \frac{r_2k_3k_5F[N_2O]_{ss}}{(k_4F + k_3)(k_5F[N_2O]_{ss} + k_6)}$$

The results of fitting the data to these equations are given in Table 2.

TABLE 3

Inoculum[a] History	Initial Cell Density (Cells/ml x 10^{-6})	Growth Rate (Cells/ml-min) x 10^{-6})	Carbon[b] Source	Initial $[NO_2^-]$ (μM)	NO[c] Yield (%)
A	*P. perfectomarina*:	--	Succinate	100	6
AN	--	--	Succinate	100	--
AN	0.21	0.100	Asparagine	100	4
AN	0.55	0.006	Asparagine	100	4
A	--	--	Broth	22.5	8
AN	0.65	--	Succinate	21.5	18
AN	0.25	0.005	Succinate	14.2	18
AN	1.00	0.007	Succinate	21.2	10
A	0.50	0.005	Succinate	15.3	15
A	0.25	0.003	Succinate	8.2	23
A	*Pa. denitrificans*: 0.80	small	Broth	19.9	21

(a) A = Aerobic; AN = anaerobic in presence of ≤100 μM $[NO_2^- + NO_3^-]$.
(b) Broth = DIFCO marine broth.
(c) As percent of nitrite reduced over central 80% of the time course. Recovered using a slightly different with F = 200 ml (STP)/min. N_2O was not measured.

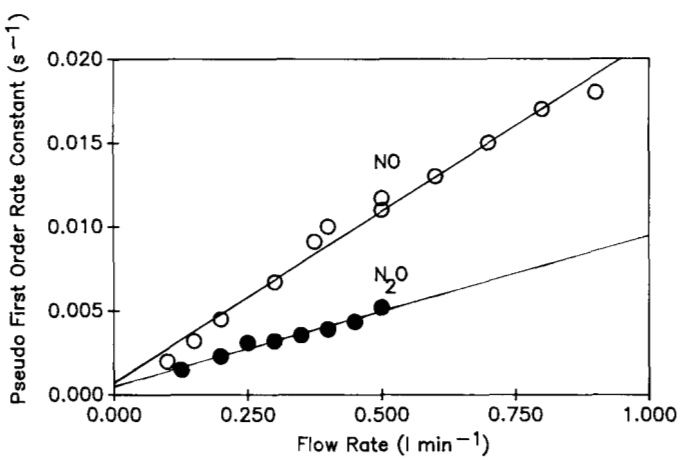

Figure 5. Data and regressions of first-order gas evolution decays versus gas sparging rate used to determine conditional stripping rate constants for nitric oxide and nitrous oxide under conditions used in this work. Slopes are reported in Table 2 as k_4 and k_5.